6838 *Biochemistry* **2010,** *49,* 6838–6845
DOI: 10.1021/bi100922r

BIOCHEMISTRY
including biophysical chemistry & molecular biology
Article

A Fluorescent Pentameric Thiophene Derivative Detects in Vitro-Formed Prefibrillar Protein Aggregates[†]

Per Hammarström, Rozalyn Simon, Sofie Nyström, Peter Konradsson, Andreas Åslund, and K. Peter R. Nilsson*

Department of Chemistry, IFM, Linköping University, SE-581 83 Linköping, Sweden

Received December 10, 2009; Revised Manuscript Received July 4, 2010

ABSTRACT: Protein aggregation is associated with a wide range of diseases, and molecular probes that are able to detect a diversity of misfolded protein assemblies are of great importance. The identification of prefibrillar states preceding the formation of well-defined amyloid fibrils is of particular interest both because of their likely role in the mechanism of fibril formation and because of the growing awareness that these species are likely to play a critical role in the pathogenesis of protein deposition diseases. Herein, we explore the use of an anionic oligothiophene derivative, p-FTAA, for detection of prefibrillar protein aggregates during in vitro fibrillation of three different amyloidogenic proteins (insulin, lysozyme, and prion protein). p-FTAA generally detected prefibrillar protein aggregates that could not be detected by thioflavine T fluorescence and in addition showed high fluorescence when bound to mature fibrils. Second, the kinetics of protein aggregation or the formation of amyloid fibrils of insulin was not extensively influenced by the presence of various concentrations of p-FTAA. These results establish the use of p-FTAA as an additional tool for studying the process of protein aggregation.

A broad range of diseases are associated with the conversion of a specific peptide or protein from its soluble functional state into highly ordered fibrillar aggregates. These pathological entities are generally described as amyloid fibrils or plaques when they accumulate extracellularly, whereas the term intracellular inclusion bodies has been suggested as being more appropriate when morphologically similar fibrils are form inside the cell (*1*). Ultrastructurally, the fibrils have a diameter of 7−10 nm, and structural studies of amyloids with high-resolution methods have typically revealed a cross-β-pleated sheet conformation. At least 25 different proteins have been reported to form disease-associated amyloids in vivo (*1*), and there is evidence that many if not all polypeptides can be induced to form amyloid in vitro (*2*).

The investigation of protein aggregation diseases and amyloid fibrils has been greatly facilitated by the development of small hydrophobic dyes that specifically bind amyloid fibrils. Green birefringence from Congo red in cross-polarized light is normally used for the visualization of amyloid plaques in tissue sections, whereas the fluorescence from thioflavins, thioflavin T (ThT)[1] or thioflavin S (ThS), is the preferable choice for monitoring amyloid formation events in the test tube. However, the utilization of the optical properties from these dyes is restricted to detecting the presence of highly regular distinct amyloid fibrils. This is a limitation of these dyes, as the full elucidation of the aggregation process of a protein requires the identification of all the conformational states and oligomeric structures adopted by the polypeptide chain during the process. It is evident that significant morphological variation can exist between different fibrils formed from the same peptide or protein and that such variation in morphology is most likely linked to heterogeneity in molecular structure, i.e., in the structural positioning of the polypeptide chains within the fibrils (*3*−*9*). Furthermore, the identification and characterization of prefibrillar states preceding the formation of well-defined fibrils are of particular interest both because of their likely role in the mechanism of fibril formation and because of the growing awareness that these species are likely to play a critical role in the pathogenesis of protein deposition diseases (*10*−*17*). However, prefibrillar states are small and metastable, making them difficult to identify in biological samples, and their structural features are difficult to determine. The only useful probes for their identification are the recently developed oligomer-specific antibodies (*18*−*20*). Hence, the development of agents for detecting prefibrillar states during the aggregation process of proteins is of great importance.

We have previously described the use of luminescent conjugated polythiophenes (LCPs) as optical probes for selective staining of protein aggregates (*21*−*27*). More recently, novel chemically defined pentameric thiophene derivatives, denoted luminescent conjugated oligothiophenes (LCOs), that could be utilized for real-time imaging of protein aggregates in vivo were developed (*28*). When the dyes bind to protein aggregates, the conformational freedom of the flexible thiophene backbone of these dyes is restricted and the emission properties of the probes are affected in a conformation-dependent manner. Hence, an optical fingerprint for distinct protein conformations can be obtained. This phenomenon has recently been used to distinguish prion strains and for discrimination of heterogeneous Aβ plaques (*24*, *25*, *27*). A pentameric thiophene derivative, 4′,3‴-bis(carboxymethyl)[2,2′;5′,2″;5″,2‴;5‴,2⁗]quinquethiophene-5,5⁗-dicarboxylic acid

[†]This work was supported by the Swedish Research Council (P.H.), the Knut and Alice Wallenberg Foundation (P.H. and P.K.), Linköping University (P.H. and P.K.), The Swedish Foundation for Strategic Research (P.H. and P.K.), and the European Union FP7 HEALTH (Project LUPAS) (K.P.R.N., P.H., A.Å., and S.N.).

*To whom correspondence should be addressed: Department of Chemistry, IFM, Linköping University, SE-581 83 Linköping, Sweden. Phone: +46 13 28 27 87. Fax: +46 13 13 75 68. E-mail: petni@ifm.liu.se.

[1]Abbreviations: LCPs, luminescent conjugated polythiophenes; LCOs, luminescent conjugated oligothiophenes; p-FTAA, 4′,3‴-bis(carboxymethyl)[2,2′;5′,2″;5″,2‴;5‴,2⁗]quinquethiophene-5,5⁗-dicarboxylic acid; ThT, thioflavin T; TEM, transmission electron microscopy; OD, optical density.

 Published on Web 07/06/2010

(p-FTAA), has also been utilized for the detection of thioflavin T negative (ThT^-) prefibrillar species during in vitro fibrillation of recombinant Aβ1−40 (*28*), indicating that LCOs might be superior to conventional amyloid ligands in identifying prefibrillar states during the fibrillation process. Herein we explore the use of p-FTAA for detection of prefibrillar protein aggregates during in vitro fibrillation of bovine insulin, hen egg lysozyme, and recombinant human prion protein. The kinetics of fibrillation were followed by p-FTAA fluorescence, ThT fluorescence, and transmission electron microscopy (TEM). p-FTAA generally bound to ThT^- prefibrillar protein aggregates that preceded the formation of mature amyloid fibrils.

METHODS

p-FTAA Synthesis and Preparation of Proteins. The synthesis of the sodium salt of p-FTAA was reported elsewhere (*28*). One milligram of p-FTAA was dissolved in 1 mL of deionized water, and this solution was further diluted with deionized water to achieve a stock solution of 15 μM p-FTAA. Bovine insulin and hen egg white lysozyme were obtained in pure form from Sigma, and the purity was assessed via SDS−PAGE. The absorbance at 280 nm was employed for concentration determinations using an ε_{280} of 5840 M^{-1} cm^{-1} and an ε_{280} of 37750 M^{-1} cm^{-1} for insulin and lysozyme, respectively. Insulin was dissolved in 2 M acetic acid (HAc) and 500 mM NaCl and stored (5 mg/mL) at 4 °C, where the solutions were stable for several weeks. Lyophilized lysozyme from hen egg white was dissolved in deionized water and dialyzed versus three changes of 25 mM HCl at 4 °C. Filtered (0.45 μm) stock solutions were made to 500 μM and stored at 4 °C. His-tagged human prion protein (HuPrP) was purified from *Escherichia coli* using Ni-NTA technology followed by size exclusion chromatography with PBS [50 mM phosphate, 100 mM NaCl, and 50 mM KCl (pH 7.3)] as the running buffer (*2*).

Amyloid Fibril Formation of Hen Egg White Lysozyme. Lysozyme amyloid-like fibrils were made through incubation of the protein (0.5 mg/mL) in 25 mM HCl at 65 °C for 3 days (*30*). Aliquots (50 μL) were withdrawn at different time points and mixed with 2 μL of the p-FTAA stock solution (15 μM) or 2 μL of a ThT stock solution (15 μM) and diluted to a final concentration of 100 μL with 25 mM HCl. The samples were prepared in microtiter plates and incubated for 10 min at room temperature. The emission spectra were recorded with a Tecan Saphire 2 plate reader. All of the spectra were recorded with excitation at 450 nm (p-FTAA) or 440 nm (ThT).

Amyloid Fibril Formation of Bovine Insulin. Amyloid fibrils of bovine insulin were prepared according to a previously reported protocol (*31*). In brief, a stock solution containing 5 mg/mL bovine insulin in 2 M acetic acid and 500 mM NaCl was placed in a water bath kept at 50 °C to induce formation of amyloid-like insulin fibrils. Aliquots (100 μL) were withdrawn at different time points and mixed with 2 μL of the p-FTAA stock solution (15 μM) or 2 μL of a ThT stock solution (15 μM). The fibrillation was also performed having 300 nM p-FTAA or ThT present during the fibrillation event. The samples were prepared in microtiter plates and incubated for 10 min at room temperature. The emission spectra were recorded as described above.

Amyloid Fibril Formation of Recombinant Human PrP-(90−231). We induced fibril formation of HuPrP under native conditions by aliquoting 800 μL of a 6 μM protein solution (50 mM phosphate, 100 mM NaCl, and 40 mM KCl) in 2 mL sealable tubes and applying 350 rpm orbital shaking at 37 °C (*34*). We sampled HuPrP by withdrawing samples at different time points, transferring aliquots to microtiter plates, and keeping them at 4 °C which prevented further fibrillation. Assay solutions containing either p-FTAA or ThT were added prior to measurement. PrP fibrils were also generated from the denatured protein. For this purpose, the protein was denatured in 6 M GdnHCl overnight and then diluted to reach a final protein concentration of 6 μM and denaturant concentrations of 1 M GdnHCl and 3 M urea in the PBS buffer previously mentioned. Samples were aliquoted and agitated according to the native protocol (*32*). PrP oligomers were generated by unfolding the protein in 10 M urea overnight followed by dilution to 5 M urea, 20 mM NaAc (pH 3.7), and 200 mM NaCl and incubation at room temperature overnight (*33*).

Transmission Electron Microscopy Experiments. Aliquots collected at different time points during fibril formation were diluted 10-fold in 25 mM HCl, and 5 μL was applied to carbon-coated grids (Carbon-B) (Pelco International, Redding, CA) for 2 min. The grids were washed and negatively stained with uranyl acetate (1%, w/v) in water and air-dried before being examined with a Jeol 1230 transmission electron microscope (TEM) at an accelerating voltage of 100 kV.

Exploring p-FTAA as an Anti-Amyloidogenic Agent. A stock solution containing 5 mg/mL bovine insulin in 2 M acetic acid and 500 mM NaCl was placed in a water bath kept at 50 °C to induce formation of amyloid-like insulin fibrils. The fibrillation was performed with 0, 0.005, 0.050, 0.500, 5, 50, and 100 μM p-FTAA; 100 μL of each sample was withdrawn at specific time points, and the optical density (OD) and p-FTAA emission were recorded with Tecan Saphire 2 plate reader. The samples were also analyzed by TEM as described above.

RESULTS

Fibrillation of Lysozyme. The time course of the nucleated conformational conversion of a peptide or protein into its fibrillar form, measured by conventional techniques, such as ThT fluorescence, typically includes a lag phase that is followed by a rapid exponential growth phase and a plateau phase (*2*, *29*). To improve our understanding of the amyloid formation event, we set out to search for small amyolid ligands that can be used as probes for identification of prefibrillar aggregates that are present during the initial lag phase. As previously reported LCPs have been shown to give kinetic information regarding in vitro amyloid formation similar to that of conventional dyes such as ThT (*21*, *22*), we decided to try the recently developed pentameric thiophene derivative, p-FTAA (Figure 1A), which has previously been shown to detect prefibrillar aggregates of the recombinant Aβ1−40 peptide (*28*).

First we compared p-FTAA with ThT using a protocol previously reported in a detailed study of the kinetics of lysozyme fibrillation (*30*). The spectra from p-FTAA alone under acidic conditions [10 mM HCl (pH 1.6)] or p-FTAA mixed with freshly dialyzed unfolded lysozyme were similar with an emission maximum around 630 nm, indicating that p-FTAA forms π-stacked aggregates under acidic conditions and that dye does not bind to the unfolded lysozyme (Figure 1B). However, already after 2 h, the emission spectrum of p-FTAA was altered and a new peak with an emission maximum around 530 nm was observed, whereas the magnitude of the peak at 630 nm decreased (Figure 1B). The new peak most likely occurred due to an interaction between p-FTAA and a prefibrillar state of lysozyme, leading to a disruption of the π-stacked aggregates. The emission at 530 nm was

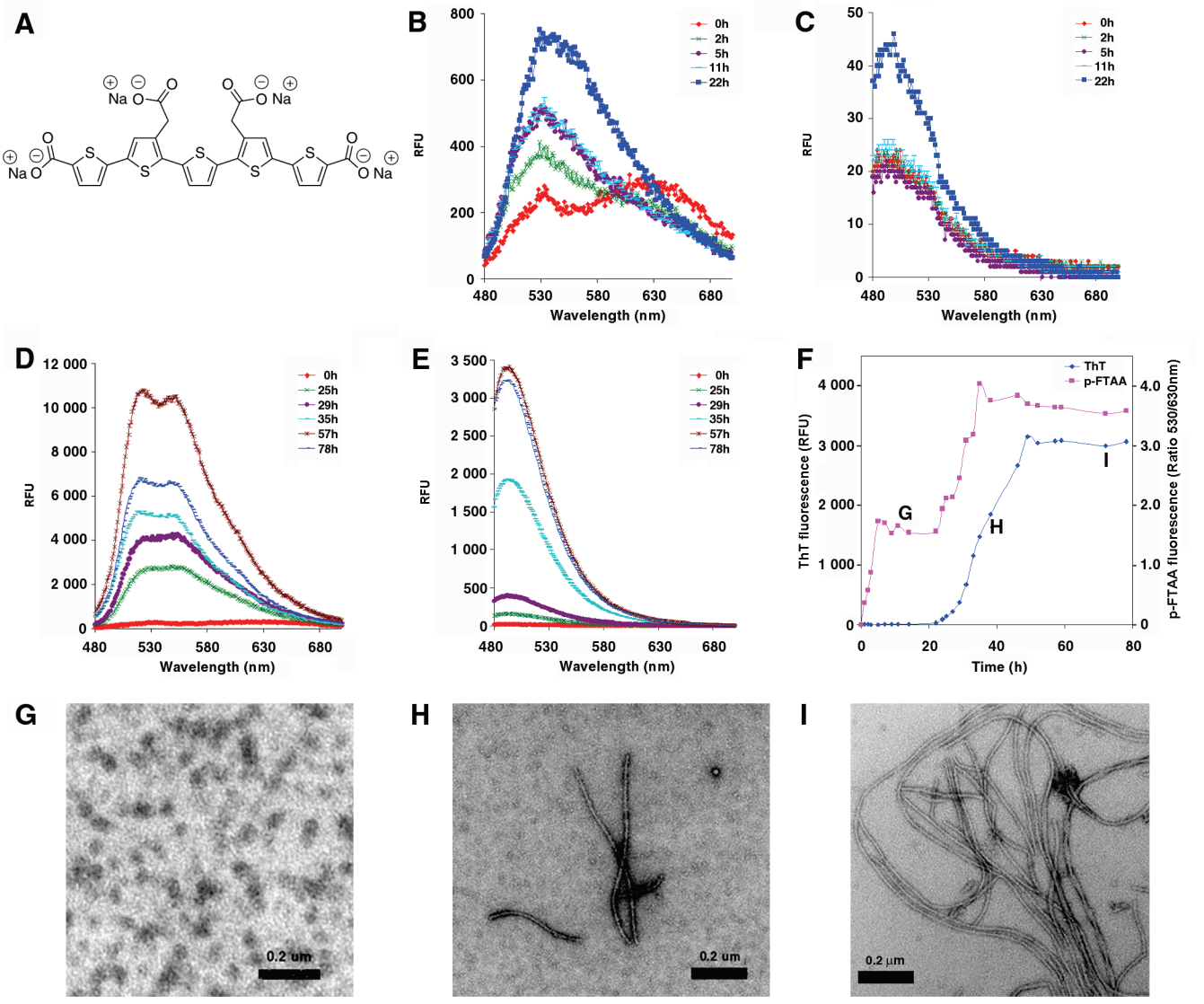

FIGURE 1: (A) Chemical structure of the sodium salt of p-FTAA. (B) p-FTAA fluorescence at early time points during fibrillation of lysozyme. (C) ThT fluorescence at early time points during fibrillation of lysozyme. (D) p-FTAA fluorescence at later time points during fibrillation of lysozyme. (E) ThT fluorescence at later time points during fibrillation of lysozyme. (F) Comparison between the kinetics of lysozyme fibrillation using p-FTAA or ThT fluorescence. (G–I) TEM micrographs of aggregated lysozyme species from samples taken during the first plateau phase observed with p-FTAA (G), the characteristic growth phase observed with ThT (H), and the final plateau phase (I).

decreased further and reached a saturation point after incubation for 5 h and stayed steady up to 22 h, where an increase in emission was observed again (Figure 1B). Interestingly, at a similar time point, the emission from ThT was slightly enhanced, suggesting that amyloid-like fibrils of lysozyme had occurred in the sample (Figure 1C). Between 25 and 50 h, the intensity of the emission from both of the dyes was increasing, and at longer incubation times, the emission of ThT was stable; on the other hand, the emission from p-FTAA was slightly decreasing because of the assembly of a higher-order aggregated form of lysozyme (Figure 1D,E). Hence, the characteristic kinetic behavior, an exponential growth phase (between 25 and 50 h) and a plateau phase (50 h), of a nucleated conformational conversion of lysozyme into amyloid-like fibrils was observed upon examination of the emission from both of the dyes. However, by plotting the ratio of the intensity of the emitted light from p-FTAA at 530 and 630 nm, we observed an additional growth phase and plateau phase prior to the normal phases visualized by ThT emission (Figure 1F). The p-FTAA$^+$ and ThT$^-$ species that were present during the earlier plateau phase were further examined by transmission electron microscopy (TEM), and as shown in Figure 1G, the predominant species during this time frame consisted of small spherical clusters of lysozyme. On the other hand, amyloid-like fibrils were observed with TEM during the ThT$^+$ growth phase and the plateau phase (Figure 1H,I). Notably, the appearance of the p-FTAA emission spectrum was significantly altered during the second exponential growth phase, and spectra with well-resolved substructure, emission maxima at 525 and 550 nm were observed (Figure 1D). Such well-resolved spectral substructures have previously been observed from p-FTAA bound to amyloid-like recombinant Aβ1–40 and Aβ1–42 fibrils and protein aggregates associated with cerebral amyloidoses and are most likely induced by the rigid fixation of the thiophene backbone upon binding within a defined fibril-binding pocket (*28*). Thus, the backbone of p-FTAA seems to be constrained in a different fashion being bound to ThT$^-$ prefibrillar states or amyloid-like fibrils of lysozyme, as the spectral substructures were not observed at earlier time points.

Fibrillation of Bovine Insulin. Next we monitored the fibrillation kinetics of insulin with p-FTAA fluorescence. Here we chose a recently reported protocol, as insulin was shown to

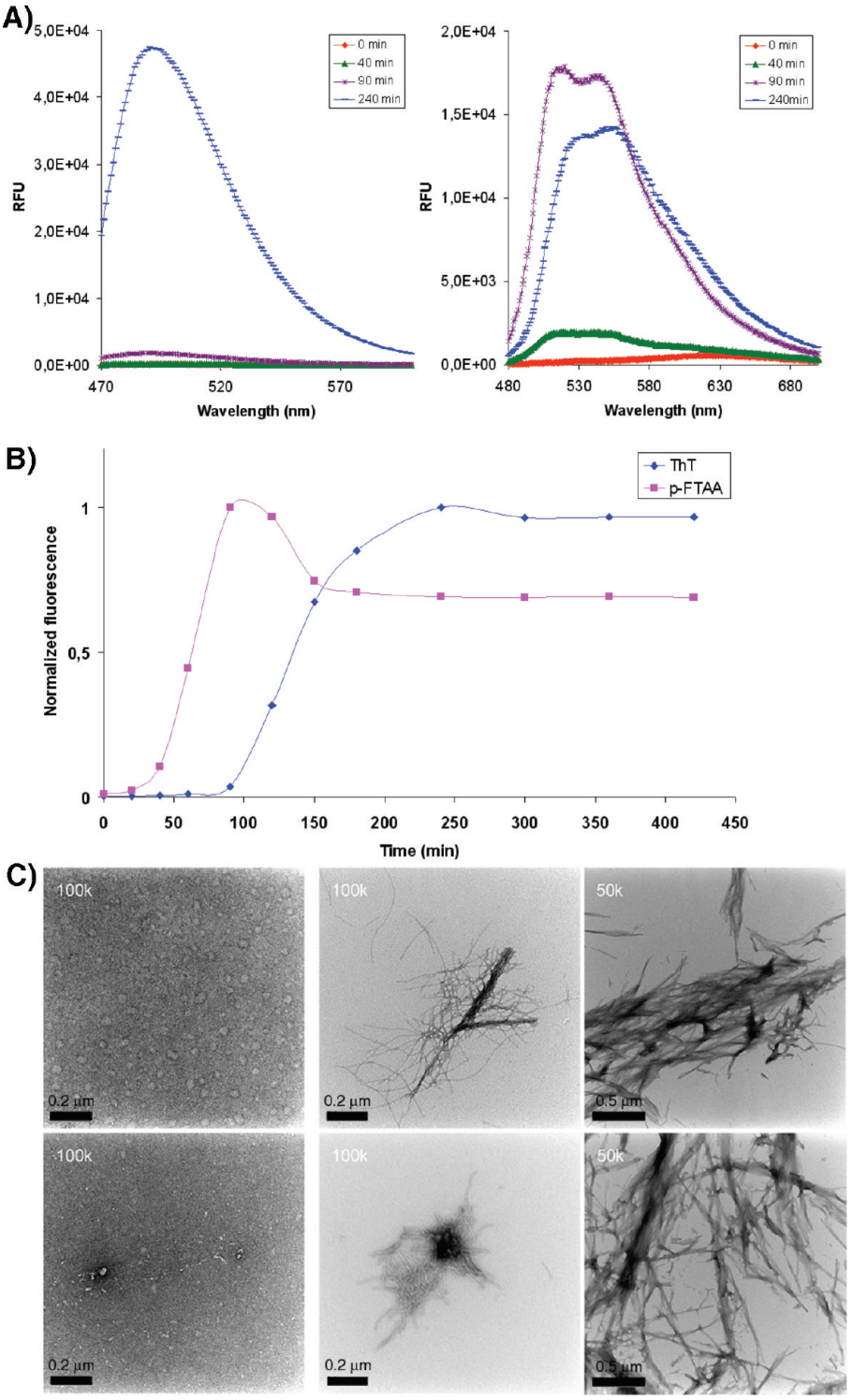

FIGURE 2: (A) ThT (left) and p-FTAA (right) fluorescence at different time points during fibrillation of insulin. (B) Comparison between the kinetics of insulin fibrillation using p-FTAA or ThT fluorescence. (C) TEM pictures of aggregated insulin species at 40 min (left), 90 min (middle), or 240 min (right) without (top row) or with (bottom row) p-FTAA during fibrillation.

assemble into amyloid fibrils through a hexameric oligomeric unit under the conditions used (*31*). Similar to the observation for lysozyme, the spectra of free p-FTAA or p-FTAA mixed with native insulin under acidic conditions were similar and showed an emission maximum at 630 nm (Figure 2A). However, already after incubation for 40 min, the spectrum of p-FTAA was altered, seen as an increased emission and a shift of the emission maximum toward shorter wavelengths (Figure 2A). At the same time point, the fluorescence of ThT was not enhanced, showing that there were no amyloid-like fibrils present in the solutions (Figure 2A). This observation was also verified by TEM, which showed only small aggregates of insulin at this time point (Figure 2C). Hence, like the observations for lysozyme fibrillation, p-FTAA interacts with prefibrillar ThT^{-} aggregates. However, the spectrum for p-FTAA bound to the prefibrillar aggregates of insulin had a more well-defined vibrational substructure, peaks at 525 and 550 nm, than the spectrum obtained from the dye bound to prefibrillar lysozyme aggregates, and the intensity

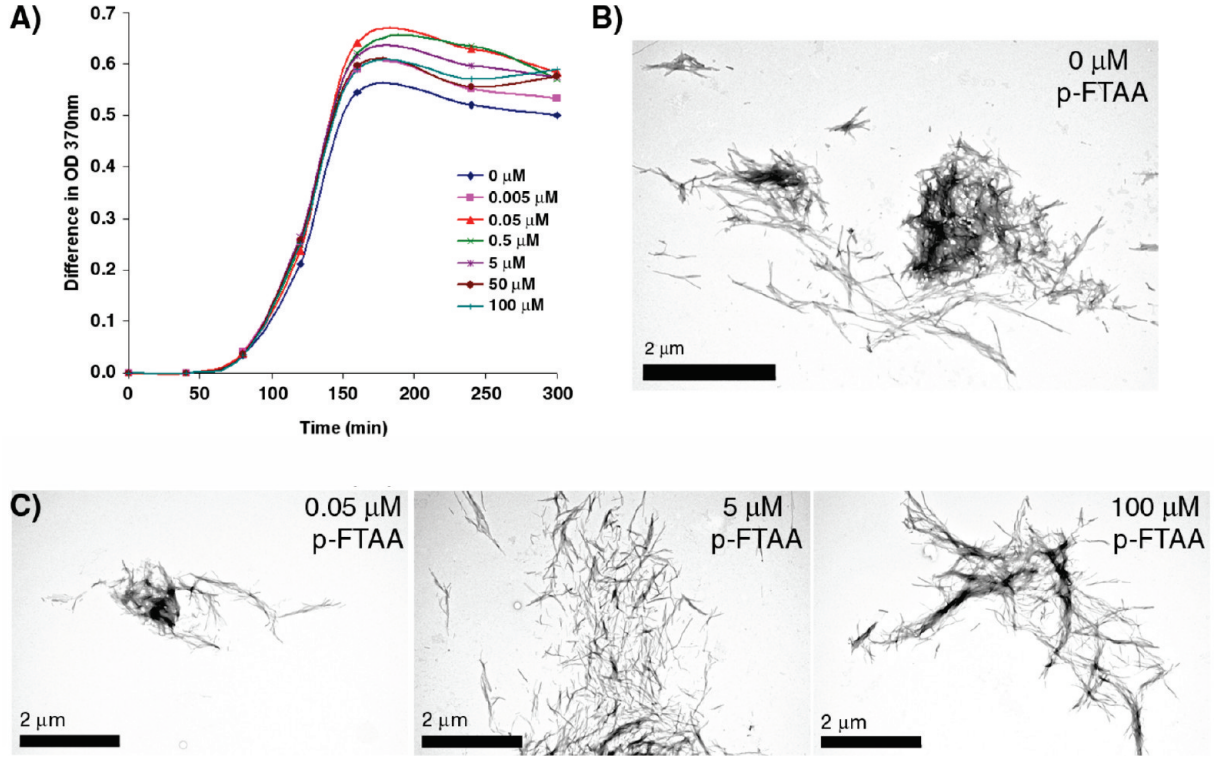

FIGURE 3: Kinetics of insulin amyloid-like fibril formation having different concentrations of p-FTAA present during the fibrillation event. The fibrillation was performed with samples with 750 μM insulin, and the samples were incubated at 50 °C in 2 M acetic acid and 0.5 M NaCl. The formation of amyloid fibrils was monitored by the difference in optical density (OD) at 370 nm (A) or TEM (B and C). The difference in OD is shown as the mean value of three independent samples for each p-FTAA concentration. The samples for TEM were taken after 240 min.

of the emission was also more pronounced. After 90 min, when both ThT fluorescence (Figure 2A) and TEM (Figure 2C) showed the presence of amyloid-like insulin fibrils in the solution, the spectrum of p-FTAA was still showing the characteristic well-defined vibrational substructure and the intensity of the emission was increased compared to that after 40 min (Figure 2A). ThT fluorescence showed that the exponential growth phase started around 90 min and the plateau phase was reached at approximately 240 min (Figure 2B). A similar plot for p-FTAA fluorescence showed an earlier onset already after 40 min, and the maximum fluorescence signal was reached after 90 min (Figure 2B). At later time points, the fluorescence decreased (Figure 2B) and the emission spectrum was slightly red-shifted (Figure 2A), indicating that p-FTAA adopts a somewhat different conformation bound to the insulin fibrils present at the different time points. A red shift of the spectrum and a decrease in the intensity of the emitted light are associated with stacking of the thiophene rings (*12*), suggesting that collateral assembly of bundles of insulin fibrils that are seen at 240 min (Figure 2C) will bring adjacent oligothiophene molecules into close contact. Amyloid fibrillation was also performed in the absence of any dye, and the results of the TEM analysis were similar to those described above (Figure 2C).

Investigation of Whether p-FTAA Influences Insulin Amyloid Fibril Formation Kinetics. As p-FTAA was found to bind to prefibrillar aggregates for a diversity of amyloidogenic proteins, it was important to investigate if p-FTAA influenced the fibril formation reaction. Therefore, we decided to perform experiments having different concentrations of p-FTAA present during the fibrillation of bovine insulin. This protocol was chosen as our model system, since the formation of insulin amyloid-like fibrils can be verified by both TEM and optical density (OD) measurements. As revealed by OD measurements, the kinetics of insulin amyloid fibril formation were not considerably altered even if 100 μM p-FTAA was present during the fibrillation event (Figure 3A). Furthermore, mature bundles of amyloid-like fibrils could also be verified by TEM in all of the samples analyzed (Figure 3B,C), suggesting that the presence of relatively large amounts p-FTAA, even though still substoichiometric, was neither blocking nor accelerating the formation of insulin amyloid fibrils under the conditions used (2 M acetic acid and 500 mM NaCl). Thus, the kinetics of formation of mature amyloid fibrils of insulin were not prevented or increased by the presence of p-FTAA.

When analyzing the p-FTAA fluorescence, we observed a similar kinetic behavior for all the concentrations used (Figure 4). At time zero, before the formation of insulin aggregates, the p-FTAA fluorescence was quenched and the emission maximum was red-shifted toward longer wavelengths, indicative of π stacking of adjacent thiophene chains, which is especially striking for the higher concentrations of p-FTAA (Figure 4B,C). Similar to what observed earlier, the intensity was increased after incubation for 40 min, and the emission maximum was shifted toward shorter wavelengths. Notably, the well-resolved spectral signature was absent in the samples with a larger amount of p-FTAA (Figure 4B,C).

Detection of ThT Negative PrP Aggregates. Finally, we selected a protein system besides Aβ1−40 (*28*) in which protein aggregates of different types can be generated at a pH more neutral than that used for lysozyme and insulin (above). We herein evaluated p-FTAA for the detection of different conformational isoforms of recombinant human prion protein 90−231 (PrP). For this purpose, we generated PrP oligomers and PrP fibrils under denaturing conditions (*32*, *33*), as well as PrP fibrils under native conditions (*34*). No fluorescence response from

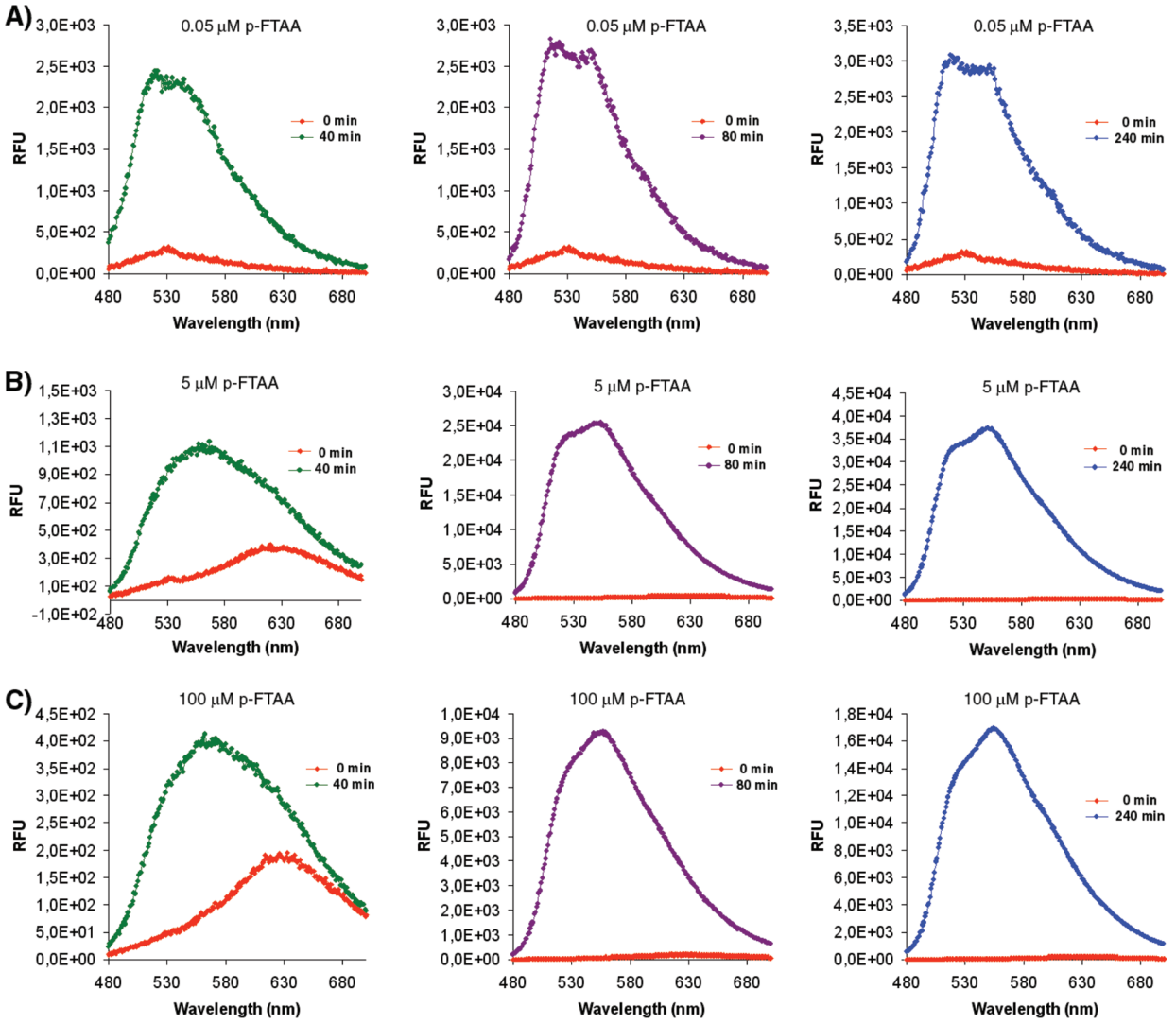

FIGURE 4: Emission spectra for different concentrations of p-FTAA at distinct time points during the fibrillation of bovine insulin. The fibrillation of insulin (5 mg/mL) was performed at 50 °C with 0.05 (A), 5 (B), or 100 μM p-FTAA (C) present during the fibrillation event.

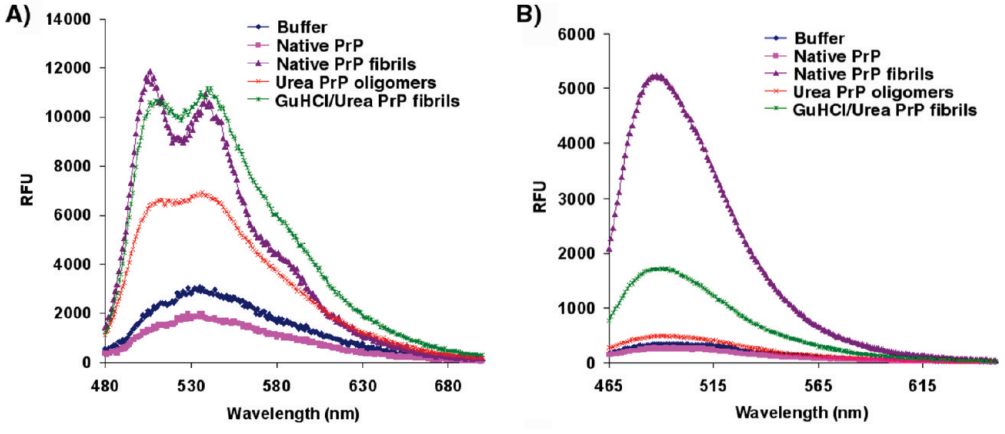

FIGURE 5: p-FTAA (A) and ThT (B) fluorescence from different in vitro preparations of recombinant human PrP 90−231. Preparations of the different PrP species are described in Methods and in refs (*32*−*34*).

p-FTAA was observed in the presence of native PrP, whereas p-FTAA exhibited an increased emission both for PrP fibrils and for oligomeric PrP (Figure 5A). An increased ThT fluorescence was only achieved for the two fibril preparations (Figure 5B) and not for the oligomers, in accordance with previous data (*35*). Hence, p-FTAA identified oligomeric PrP aggregates that were not observed by ThT fluorescence. Notably, this preparation protocol for PrP oligomers has previously been shown of to be the most potent activator of the innate immune complement system as compared to native PrP and fibrillar PrP (*35*), implying that p-FTAA recognizes a relevant biological active form of PrP of these otherwise synthetically prepared oligomers.

DISCUSSION

The identification of prefibrillar states preceding the formation of well-defined amyloid fibrils is of enormous interest both because of their likely role in the mechanism of fibril formation and because of the growing awareness that such species are likely to play a critical role in the pathogenesis of protein deposition diseases, especially neurodegenerative cerebral amyloidoses such as Alzheimer's disease and prion diseases (*10*−*17*). The finding that specific antibodies can bind to prefibrillar states from different sources, but not to their corresponding monomeric or fibrillar states, suggests that these aggregated species have similar common structural elements (*18*). Despite the precise role played by prefibrillar aggregates in the overall process of fibril formation, the identification of such species is crucial as these species could be the primary toxic agents involved in neurodegenerative disorders (*13*−*15*). Small amyloid ligands, such as thioflavins or derivatives of Congo red, can reliably identify the presence of amyloid fibrils but are limited in detecting prefibrillar aggregates. Therefore, it would be desirable to expand the arsenal of amyloid ligands available for the detection of prefibrillar aggregates, and here we exploited the unique opto-physical properties of an anionic pentameric thiophene derivative, p-FTAA, to identify prefibrillar states preceding the formation of amyloid fibrils.

As we demonstrated, p-FTAA can be used as an optical tool for identifying prefibrillar species of lysozyme, insulin, and PrP. Besides its obvious practical usefulness for studying the fibrillation process of proteins, p-FTAA might be used as a scaffold for the development of sensitive detectors for protein aggregates that can be utilized for clinical diagnostics of protein misfolding and aggregation disorders. In tissue sections, p-FTAA appears to bind preferentially to protein aggregates with repetitive cross-β-sheet structures, whereas other molecules physiologically present in the tissue are left unstained (*28*, *36*). Furthermore, other thiophene-based LCPs have shown to identify both nonthioflavinophilic and noncongophilic prion aggregates (*25*, *27*). This could mean that LCO or LCP fluorescence yields stronger signals than thioflavin T and Congo red birefringence, resulting in higher sensitivity and detection of deposits that would have gone undetected with other conventional amyloid ligands. Alternatively, the collection of aggregate topologies identified by the LCOs and LCPs may include a subset of those that can be stained with thioflavin T or Congo red as well as deposits not formally qualifying as amyloid. Whether the LCOs better performance in identifying proteins deposits is due to higher sensitivity or to elementary differences in the biophysical nature of the detected protein deposits, it seems to be a general mechanism for a variety of proteins. A repetitive thiophene core motif seems to be a preferable structure for obtaining high-affinity amyloid ligands, and except for LCPs and LCOs, other ligands with shorter thiophene cores have been reported (*37*, *38*). Hence, it would be of great interest to explore LCOs with different lengths of the repetitive thiophene core motif, and such experiments are ongoing in our laboratories.

Exploring LCOs with distinct amounts of thiophene moieties would also be essential for understanding the fundamental spectral properties of these molecules that are achieved upon interaction with protein aggregates. This understanding is highly significant for taking full advantage of the conformation-dependent optical information that can be achieved from the LCOs when analyzing the spectral data obtained from the dyes bound to protein aggregates. Both LCPs and LCOs have previously been proven to be useful for spectral distinction of heterogenic populations of protein aggregates (*24*, *25*, *28*) and for spectral assignment of distinct types of protein aggregates (*36*, *39*). Herein, we also observed some indications that a certain spectroscopic signature might be associated with a distinct prefibrillar species. However, the spectral signature from p-FTAA bound to a distinct aggregated species was also highly dependent on the concentration of dye used. It is important to emphasize that the spectral signature from p-FTAA is only an indirect read-out of the morphology or conformation of the aggregated proteinaceous species that is targeted by the dye, and as shown previously (*28*), the side chain functionalizations and the positioning of these groups are also important in obtaining a spectral distinction between distinct protein aggregates. Hence, creating a molecularly diverse library of LCOs, having a certain amount of repetitive thiophene units and proper side chain functionalization, and screening this library for distinct amyloid molecular targets are essential for gaining further insights regarding the spectral signatures achieved from LCOs bound to distinct protein aggregates.

We also explored if p-FTAA interfered with the protein aggregation process. Notably, relatively high concentrations of p-FTAA did not seem to influence the kinetics or formation of insulin amyloid fibrils under the acidic conditions used herein. Apparently, the driving force for amyloid formation of insulin under these conditions is dictated by the strong affinity between insulin molecules to form the cross-β-sheet structure. Our results should be taken with caution; the acidic conditions used lead to protonation of p-FTAA, resulting in strong affinity between p-FTAA molecules as noted by the red-shifted fluorescence of the free dye under these conditions. Hence, the probed concentrations up to a stoichiometry of $^1/_8$ of that of insulin are likely less available for binding to insulin than forming an assembly of stacked LCOs. This in addition indicates that for p-FTAA a micellar inhibitory effect like that previously described for in vitro amyloid suppressors (*40*) cannot efficiently cap a growing insulin fibril under the conditions used. These data do by all means rule out the possibility that p-FTAA might serve as a pharmacophore for developing therapeutically active agents for protein aggregation diseases. In particular, it is obvious that p-FTAA strikes at the pathological hallmarks, i.e., protein deposits, of these diseases (*28*, *35*). As p-FTAA in addition targets prefibrillar species, minor alterations of the molecular structures in a similar fashion to β-sheet breaking peptides (*41*, *42*) might efficiently prevent the amyloid fibril formation or block the toxicity of the prefibrillar species.

In conclusion, we have shown that a pentameric thiophene derivative, p-FTAA, can be utilized for the detection of prefibrillar nonthioflavinophilic protein aggregates during in vitro fibrillation of a variety of amyloidogenic proteins. We foresee that p-FTAA will be utilized as an additional tool for studying the formation of protein aggregates and serve as a molecular scaffold for expanding the toolbox of amyloid ligands.

ACKNOWLEDGMENT

We thank Mikael Lindgren for helpful discussions about fluorescence spectroscopy.

REFERENCES

1. Westermark, P., Benson, M. D., Buxbaum, J. N., Cohen, A. S., Frangione, B., Ikeda, S., Masters, C. L., Merlini, G., Saraiva, M. J., and Sipe, J. D. (2007) A primer of amyloid nomenclature. *Amyloid 14*, 179–183.
2. Chiti, F., and Dobson, C. M. (2006) Protein misfolding, functional amyloid, and human disease. *Annu. Rev. Biochem. 75*, 333–366.

3. Bauer, H. H., Aebi, U., Haner, M., Hermann, R., Muller, M., and Merkle, H. P. (1995) Architecture and polymorphism of fibrillar supramolecular assemblies produced by in vitro aggregation of human calcitonin. *J. Struct. Biol. 115*, 1–15.
4. Jimenez, J. L., Guijarro, J. I., Orlova, E., Zurdo, J., Dobson, C. M., Sunde, M., and Saibil, H. R. (1999) Cryo-electron microscopy structure of an SH3 amyloid fibril and model of the molecular packing. *EMBO J. 18*, 815–821.
5. Jimenez, J. L., Nettleton, E. J., Bouchard, M., Robinson, C. V., Dobson, C. M., and Saibil, H. R. (2002) The protofilament structure of insulin amyloid fibrils. *Proc. Natl. Acad. Sci. U.S.A. 99*, 9196–9201.
6. Petkova, A. T., Leapman, R. D., Guo, Z., Yau, W. M., Mattson, M. P., and Tycko, R. (2005) Self-propagating, molecular-level polymorphism in Alzheimer's β-amyloid fibrils. *Science 307*, 262–265.
7. Pedersen, J. S., Dikov, D., Flink, J. L., Hjuler, H. A., Christiansen, G., and Otzen, D. E. (2006) The changing face of glucagon fibrillation: Structural polymorphism and conformational imprinting. *J. Mol. Biol. 355*, 501–523.
8. Sawaya, M. R., Sambashivan, S., Nelson, R., Ivanova, M. I., Sievers, S. A., Apostol, M. I., Thompson, M. J., Balbirnie, M., Wiltzius, J. J., McFarlane, H. T., Madsen, A. Ø., Riekel, C., and Eisenberg, D. (2007) Atomic structures of amyloid cross-β spines reveal varied steric zippers. *Nature 447*, 453–457.
9. Paravastu, A. K., Leapman, R. D., Yau, W. M., and Tycko, R. (2008) Molecular structural basis for polymorphism in Alzheimer's β-amyloid fibrils. *Proc. Natl. Acad. Sci. U.S.A. 105*, 18349–18354.
10. McLean, C. A., Cherny, R. A., Fraser, F. W., Fuller, S. J., Smith, M. J., Beyreuther, K., Bush, A. I., and Masters, C. L (1999) Soluble pool of Aβ amyloid as a determinant of severity of neurodegeneration in Alzheimer's disease. *Ann. Neurol. 46*, 860–866.
11. Hardy, J., and Selkoe, D. J. (2002) The amyloid hypothesis of Alzheimer's disease: Progress and problems on the road to therapeutics. *Science 297*, 353–356.
12. Chromy, B. A., Nowak, R. J., Lambert, M. P., Viola, K. L., Chang, L., Velasco, P. T., Jones, B. W., Fernandez, S. J., Lacor, P. N., Horowitz, P., Finch, C. E., Krafft, G. A., and Klein, W. L. (2003) Self-assembly of Aβ(1−42) into globular neurotoxins. *Biochemistry 42*, 12749–12760.
13. Glabe, C. G. (2006) Common mechanisms of amyloid oligomer pathogenesis in degenerative disease. *Neurobiol. Aging 27*, 570–575.
14. Cole, G. M., and Frautschy, S. A. (2006) Alzheimer's amyloid story finds its star. *Trends Mol. Med. 12*, 395–396.
15. Lesné, S., Koh, M. T., Kotilinek, L., Kayed, R., Glabe, C. G., Yang, A., Gallagher, M., and Ashe, K. H. (2006) A specific amyloid-β protein assembly in the brain impairs memory. *Nature 440*, 352–357.
16. Haass, C., and Selkoe, D. J. (2007) Soluble protein oligomers in neurodegeneration: Lessons from the Alzheimer's amyloid β-peptide. *Nat. Rev. Mol. Cell Biol. 8*, 101–112.
17. Lesné, S., Kotilinek, L., and Ashe, K. H. (2008) Plaque-bearing mice with reduced levels of oligomeric amyloid-β assemblies have intact memory function. *Neuroscience 151*, 745–749.
18. Kayed, R., Head, E., Thompson, J. L., McIntire, T. M., Milton, S. C., Cotman, C. W., and Glabe, C. G. (2003) Common structure of soluble amyloid oligomers implies common mechanism of pathogenesis. *Science 300*, 486–489.
19. Kayed, R., and Glabe, C. G. (2006) Conformation-dependent anti-amyloid oligomer antibodies. *Methods Enzymol. 413*, 326–344.
20. Lambert, M. P., Velasco, P. T., Chang, L., Viola, K. L., Fernandez, S., Lacor, P. N., Khuon, D., Gong, Y., Bigio, E. H., Shaw, P., De Felice, F. G., Krafft, G. A., and Klein, W. L. (2007) Monoclonal antibodies that target pathological assemblies of Aβ. *J. Neurochem. 100*, 23–35.
21. Nilsson, K. P. R., Herland, A., Hammarström, P., and Inganäs, O. (2005) Conjugated polyelectrolytes: Conformation-sensitive optical probes for detection of amyloid fibril formation. *Biochemistry 44*, 3718–3724.
22. Herland, A.; et al. (2005) Synthesis of a regioregular zwitterionic conjugated oligoelectrolyte, usable as an optical probe for detection of amyloid fibril formation at acidic pH. *J. Am. Chem. Soc. 127*, 2317–2323.
23. Nilsson, K. P. R.; et al. (2006) Conjugated polyelectrolytes: Conformation-sensitive optical probes for staining and characterization of amyloid deposits. *ChemBioChem 7*, 1096–1104.
24. Nilsson, K. P. R.; et al. (2007) Imaging distinct conformational states of amyloid-β fibrils in Alzheimer's disease using novel luminescent probes. *ACS Chem. Biol. 2*, 553–560.
25. Sigurdson, C. J.; et al. (2007) Prion strain discrimination using luminescent conjugated polymers. *Nat. Methods 4*, 1023–1030.
26. Åslund, A.; et al. (2007) Studies of luminescent conjugated polythiophene derivatives: Enhanced spectral discrimination of protein conformational states. *Bioconjugate Chem. 18*, 1860–1868.
27. Sigurdson, C. J., Nilsson, K. P. R., Hornemann, S., Heikenwalder, M., Manco, G., Schwarz, P., Ott, D., Rülicke, T., Liberski, P. P., Julius, C., Falsig, J., Stitz, L., Wüthrich, K., and Aguzzi, A. (2009) De novo generation of a transmissible spongiform encephalopathy by mouse transgenesis. *Proc. Natl. Acad. Sci. U.S.A. 106*, 304–309.
28. Åslund, A.; et al. (2009) Novel pentameric thiophene derivatives for in vitro and in vivo optical imaging of a plethora of protein aggregates in cerebral amyloidoses. *ACS Chem. Biol. 4*, 673–684.
29. Serio, T. R.; et al. (2000) Nucleated conformational conversion and the replication of conformational information by a prion determinant. *Science 289*, 1317–1321.
30. Mishra, R., Sörgjerd, K., Nyström, S., Nordigarden, A., Yu, Y.-C., and Hammarström, P. (2006) Lysozyme amyloidogenesis is accelerated by specific nicking and fragmentation but decelerated by intact protein binding and conversion. *J. Mol. Biol. 366*, 1029–1044.
31. Vestergaard, B., Groenning, M., Roessle, M., Kastrup, J. S., van de Weert, M., Flink, J. M., Frokjaer, S., Gajhede, M., and Svergun, D. I. (2007) A helical structural nucleus is the primary elongating unit of insulin amyloid fibrils. *PLoS Biol. 5*, e134.
32. Bocharova, O. V., Breydo, L., Parfenov, A. S., Salnikov, V. V., and Baskakov, I. V. (2005) In vitro conversion of full-length mammalian prion protein produces amyloid form with physical properties of PrP(Sc). *J. Mol. Biol. 346*, 645–659.
33. Baskakov, I. V., Legname, G., Baldwin, M. A., Prusiner, S. B., and Cohen, F. E. (2002) Pathway complexity of prion protein assembly into amyloid. *J. Biol. Chem. 277*, 21140–21148.
34. Almstedt, K., Nyström, S., Nilsson, K. P. R., and Hammarström, P. (2009) Amyloid fibrils of human prion protein are spun and woven from morphologically disordered aggregates. *Prion 3*, 224–235.
35. Sjöberg, A. P., Nyström, S., Hammarström, P., and Blom, A. M. (2008) Native, amyloid fibrils and β-oligomers of the C-terminal domain of human prion protein display differential activation of complement and bind C1q, factor H and C4b-binding protein directly. *Mol. Immunol. 45*, 3213–3221.
36. Nilsson, K. P. R., Ikenberg, K., Åslund, A., Fransson, S., Konradsson, P., Röcken, C., Moch, H., and Aguzzi, A. (2010) Structural typing of systemic amyloidoses by luminescent-conjugated polymer spectroscopy. *Am. J. Pathol. 176*, 563–574.
37. Nesterov, E. E., Skoch, J., Hyman, B. T., Klunk, W. E., Bacskai, B. J., and Swager, T. M. (2005) In vivo optical imaging of amyloid aggregates in brain: Design of fluorescent markers. *Angew. Chem., Int. Ed. 44*, 5452–5456.
38. Cui, M. C., Li, Z. J., Tang, R. K., and Liu, B. L. (2010) Synthesis and evaluation of novel benzothiazole derivatives based on the bithiophene structure as potential radiotracers for β-amyloid plaques in Alzheimer's disease. *Bioorg. Med. Chem. 18*, 2777–2784.
39. Berg, I., Nilsson, K. P. R., Thor, S., and Hammarström, P. (2010) Efficient imaging of amyloid deposits in *Drosophila* models of human amyloidoses. *Nat. Protoc. 5*, 935–944.
40. Feng, B. Y., Toyama, B. H., Wille, H., Colby, D. W., Collins, S. R., May, B. C., Prusiner, S. B., Weissman, J., and Shoichet, B. K. (2008) Small-molecule aggregates inhibit amyloid polymerization. *Nat. Chem. Biol. 4*, 197–199.
41. Soto, C., Sigurdsson, E. M., Morelli, L., Kumar, A., Castaño, E. M., and Frangione, B. (1998) β-Sheet breaker peptides inhibit fibrillogenesis in a rat brain model of amyloidosis: Implications for Alzheimer's therapy. *Nat. Med. 4*, 822–826.
42. Soto, C., Kascsak, R. J., Saborio, G. P., Aucouturier, P., Wisniewski, T., Prelli, F., Kascsak, R., Mendez, E., Harris, D. A., Ironside, J., Tagliavini, F., Carp, R. I., and Frangione, B. (2000) Reversion of prion protein conformational changes by synthetic β-sheet breaker peptides. *Lancet 355*, 192–197.